

ISOTOPIC U-Pb-SHRIMP DATING OF MUGODZHARI ECLOGITES (KAZAKHSTAN)

© 2025 K. S. Ivanov^a, V. S. Ponomarev^{a, *},

Corresponding Member of RAS V. N. Puchkov^a, and D. A. Khanin^b

Received August 19, 2024

Revised September 10, 2024

Accepted September 16, 2024

Abstract. In the extreme south of the Urals, zircons from eclogites and amphibolite were dated in metamorphites of the East Mugodzhari zone. Of the 4 eclogite samples, close (and the most “ancient” – 520 ± 4 Ma) concordant age values were obtained in 3 samples, which probably corresponds to the age of the protolith. Concordant dates of 472 ± 3 Ma and 379 ± 3 Ma reflect the time of the main stages of metamorphism of the East Mugodzhari, the more ancient relate to high-pressure, and the latter to amphibolite facies metamorphism. The presence of ancient and at the same time different-aged zircons, probably with traces of rounding, indicates the primary sedimentary nature of the studied amphibolites. The youngest zircons from the Mugodzhari eclogites have an age of 282 ± 2 Ma, corresponding to the collision stage. The obtained data show that the Mugodzhari metamorphic complexes are not Early Proterozoic or Riphean formations (as was previously believed), but represent Lower-Middle Paleozoic complexes of the middle part of the earth’s crust. That is, these metamorphites by their nature are fragments of the deep part of the island-arc system of the eastern sector of the Urals, which were later brought to a near-surface level during the rise and erosion of individual regions of the Urals.

Keywords : eclogite, amphibolite, zircon, U–Pb age, Mugodzhary, Urals, Kazakhstan

DOI: 10.31857/S26867397250103e1

The eclogites of the Eastern Mugodzhary are located in the southernmost part of the Ural fold belt, in Kazakhstan. Here, in the western part of the East Mugodzhari zone, the Taldyk sialic block is located (Fig. 1), which contacts along faults with the basic volcanics of the West Mugodzhari zone of the Magnitogorsk megazone to the west, and with the Balkymbai near-strike graben to the east. The Taldyk block is composed of metamorphic rocks predominantly of amphibolite facies, which host massifs of granites, granodiorites, and others. Among the metamorphites, the Taldyk and South Mugodzhari series are usually distinguished, subdivided into several strata [2, 10, 13], which include mainly mica gneisses, crystalline schists with kyanite and garnet, interlayers of quartzites, amphibolites,

amphibole gneisses, often migmatized, and others. The metamorphism of these strata at the progressive stage corresponded to the high-temperature ($T = 680\text{--}720^\circ\text{C}$; $P = 7\text{--}8.5$ kbar), and at the regressive stage to the low-temperature ($T = 580\text{--}630^\circ\text{C}$; $P = 5.5\text{--}6.5$ kbar) zones of amphibolite facies [4, 14]. The age of the metamorphic strata of the Taldyk block has been the subject of lengthy discussion. They were usually considered Early Proterozoic ([13] et al.), opinions about their Riphean [2, 4] or Early-Middle Paleozoic age [5] were also expressed. However, there have been practically no modern geochronological studies here, and the data [8, 9], unfortunately, were not linked to the geology of the region. Within the Taldyk block, high-pressure rocks such as two-mica kyanite-garnet schists (among which there are kyanite deposits), eclogites and eclogite-like rocks have been described [1, 13, 15]. The Mugodzhari eclogites are usually divided into two complexes – Tulepsay and Kitarsay [4, 13, 14, 16]. The Kitarsay complex (eclogite-peridotite ophiolite association) consists of numerous small bodies confined to a linear zone of northeast strike

^aZavaritsky Institute of Geology and Geochemistry, Ural Branch of the Russian Academy of Sciences, Ekaterinburg, Russian Federation

^bKorzhinskii Institute of Experimental Mineralogy, Russian Academy of Sciences, Chernogolovka, Russian Federation

*e-mail: p123v@yandex.ru

(Bugetysay fault), traced for 25 km. This zone has a thickness of up to 1 km and is composed mainly of quartz-feldspar blastomylonites of staurolite facies. The bodies (boudins, lenses) of the Kitarsay eclogite-peridotite association are located on the left bank of the Uly-Taldyk River (Fig. 1), they range in size from several meters to the first hundreds of meters. Usually they are composed of serpentinites, which contain inclusions of garnet serpentinites, websterites, eclogites, eclogite-like rocks, garnetites, and garnet amphibolites. Temperatures calculated for metabasic parageneses are 600–850°C and higher, and pressures are estimated as 7–14 kbar

[13]. Eclogite and eclogite-symplectite bodies of the Tulepsai complex are located (Fig. 1) among amphibolites on the right bank of the Tulepsai River [4, 13]. Recently, A.V. Ryazantsev and colleagues obtained a U-Pb age (SHRIMP II) from zircons of 374–372 Ma and a U-Pb age from rutile of 360 Ma from eclogites of the Tulepsai complex. The date of 374 Ma is estimated [15] as the age of eclogite facies metamorphism (with maximum parameters $P = 15$ kbar, $T = 700–750^{\circ}\text{C}$). These authors associate the date of 360 Ma with a later transformation of eclogites under decreasing pressure.

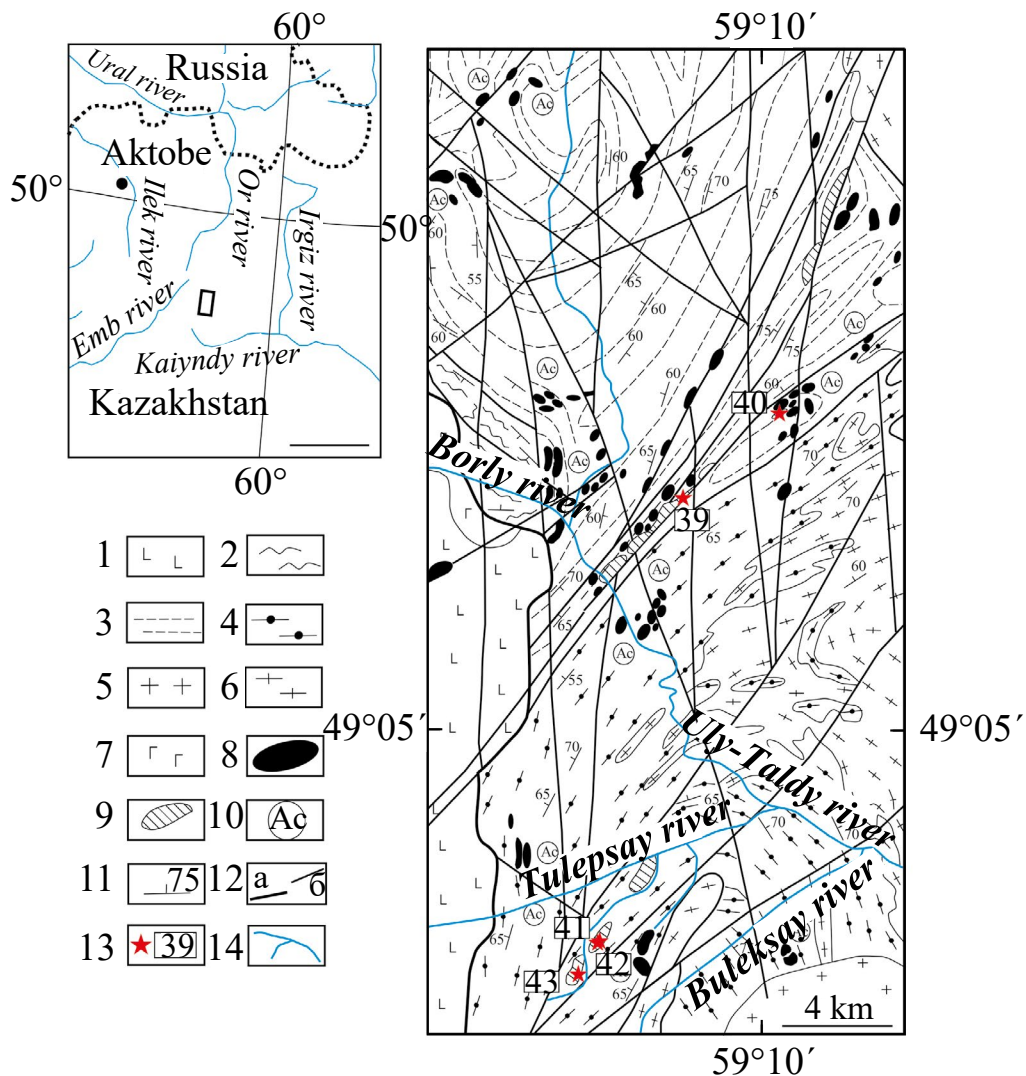


Fig. 1. Scheme of high-pressure and ultrabasic complexes distribution in the central part of the Taldyk sialic block of Mugodzhari (based on data from [1, 13, 16], with authors' modifications). 1 – basalts (D_2); 2–4 – metamorphites: quartz-phyllite series; 3 – gneiss-shale series; 4 – gneiss-amphibolite series; 5 – granites (C_2 – P_1); 6 – plagiogneiss-granites (D); 7 – gabbro, gabbro-norites (D_2); 8 – ultrabasic rocks; 9 – eclogites and eclogite-like rocks; 10 – locations of asbestized ultrabasic rock bodies; 11 – elements of schistosity occurrence; 12 – faults: main (a), secondary (b); 13 – sampling locations for dating and their numbers; 14 – rivers and streams.

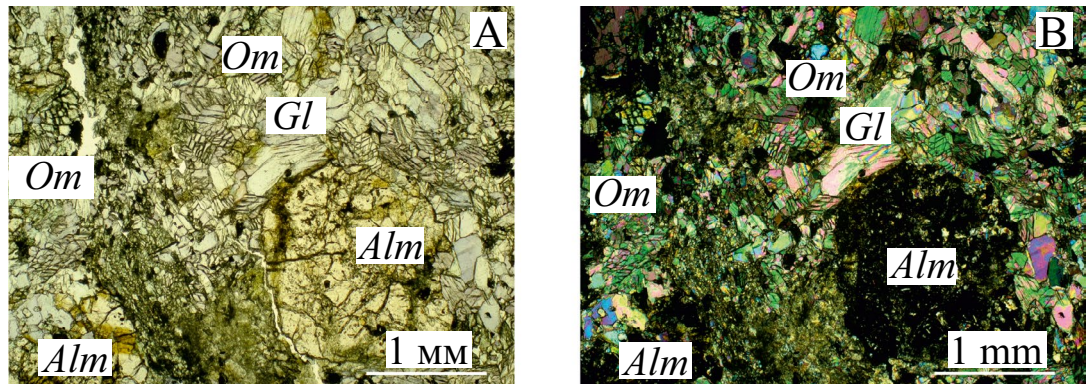


Fig. 2. Eclogite of the Tulepsay complex of the Eastern Mugodzhari (sample 41). In transmitted light (A), in polarized light (B). Alm – almandine, Om – omphacite, Gl – glaucophane.

For isotope-geochronological studies, 4 samples of eclogites and 1 sample of amphibolites were collected (see Fig. 1), each weighing more than 30 kg. The samples were taken from the central, least altered parts of boudin-shaped eclogite bodies exposed by trenches dug by the Priuralskaya team of PGO “Zapkazgeologiya” (team chief B.F. Ivanshin). Zircon separation was carried out according to standard methodology, including crushing the sample to a fraction < 0.4 mm, washing the crushed material in water to gray concentrate, magnetic separation, separation in heavy liquids, and manual selection of zircon grains under a binocular microscope. The size of the isolated zircons ranged from 100 to 350 μm . U-Th-Pb geochronological studies of zircons from eclogites were performed by A.N. Larionov on a SHRIMP-II secondary ion microprobe at the VSEGEI Research Center using the methodology described in [20]. The intensity of the primary beam of molecular negatively charged oxygen ions was $\sim 2.5\text{--}4$ nA, with a spot (crater) diameter of $\sim 15 \cdot 10 \mu\text{m}$. Individual errors are given for the 1σ (%) interval, calculated ages – 2σ (Ma). The obtained data were processed using SQUID and ISOPLOT software [19].

MATERIAL COMPOSITION OF ECLOGITES

The studied eclogites are represented by fine-grained to very fine-grained aggregate of glaucophane, omphacite, and almandine porphyroblasts (Fig. 2 A, B, sample 41). The rocks contain veins filled with omphacite, epidote, zoisite, clinzozoisite, second-generation glaucophane, and albite. The rock structure varies from fine-grained to very fine-grained, porphyroblastic, granonematoblastic, with a massive texture. The

main rock-forming minerals are omphacite, almandine, and glaucophane. Secondary minerals include: actinolite, zoisite, clinzozoisite, calcite, paragonite, ferropargasite, ferro-edenite, clinochlore, chamosite, muscovite (phengite), quartz, rutile, titanite, fluorapatite, ilmenite, albite, pyrite, zircon, and allanite-(Ce). The chemical composition of minerals and their crystal-chemical recalculations are given in Appendix 1.

Garnet in eclogites forms metacrystals (up to 1 cm) with inclusions of omphacite, actinolite, ferropargasite, ferroedenite, glaucophane, ilmenite, titanite, rutile, and fluorapatite. In terms of chemical composition, the garnet corresponds to almandine

$\text{Alm}_{59.8\text{--}72.9} \text{Prp}_{9.28\text{--}17.8} \text{Grs}_{12.3\text{--}26.7} \text{Sps}_{0.4\text{--}2.0} \text{And}_{0\text{--}1.5}$. In almandine, a slight increase in MgO content and decrease in CaO from the center to the periphery of the crystals is observed. *Glaucophane* (up to 50% of the rock volume) is the main mineral of eclogites. Relict grains of omphacite, partially replaced by clinzozoisite, titanite, and paragonite, are found in the glaucophane aggregate. The magnesium content of glaucophane ($\text{Mg}^{\#}$) is 0.64–0.73. *Omphacite* (20–30% of the rock volume) is represented by a fine-grained aggregate around almandine porphyroblasts. The jadeite mineral content in omphacite ranges from 39 to 47%. In the omphacite-glaucophane aggregate, symplectites are found, the matrix of which is represented by albite (Ab_{99}) with actinolite inclusions. A fine-grained albite-clinochlore-chamosite aggregate with phengite is noted around large almandine porphyroblasts in the rocks. Zoisite in the rocks overgrows small elongated individuals of glaucophane. Some zoisite grains in the glaucophane-omphacite aggregate are replaced by clinzozoisite at the periphery. Also, clinzozoisite individuals are noted in the rocks,

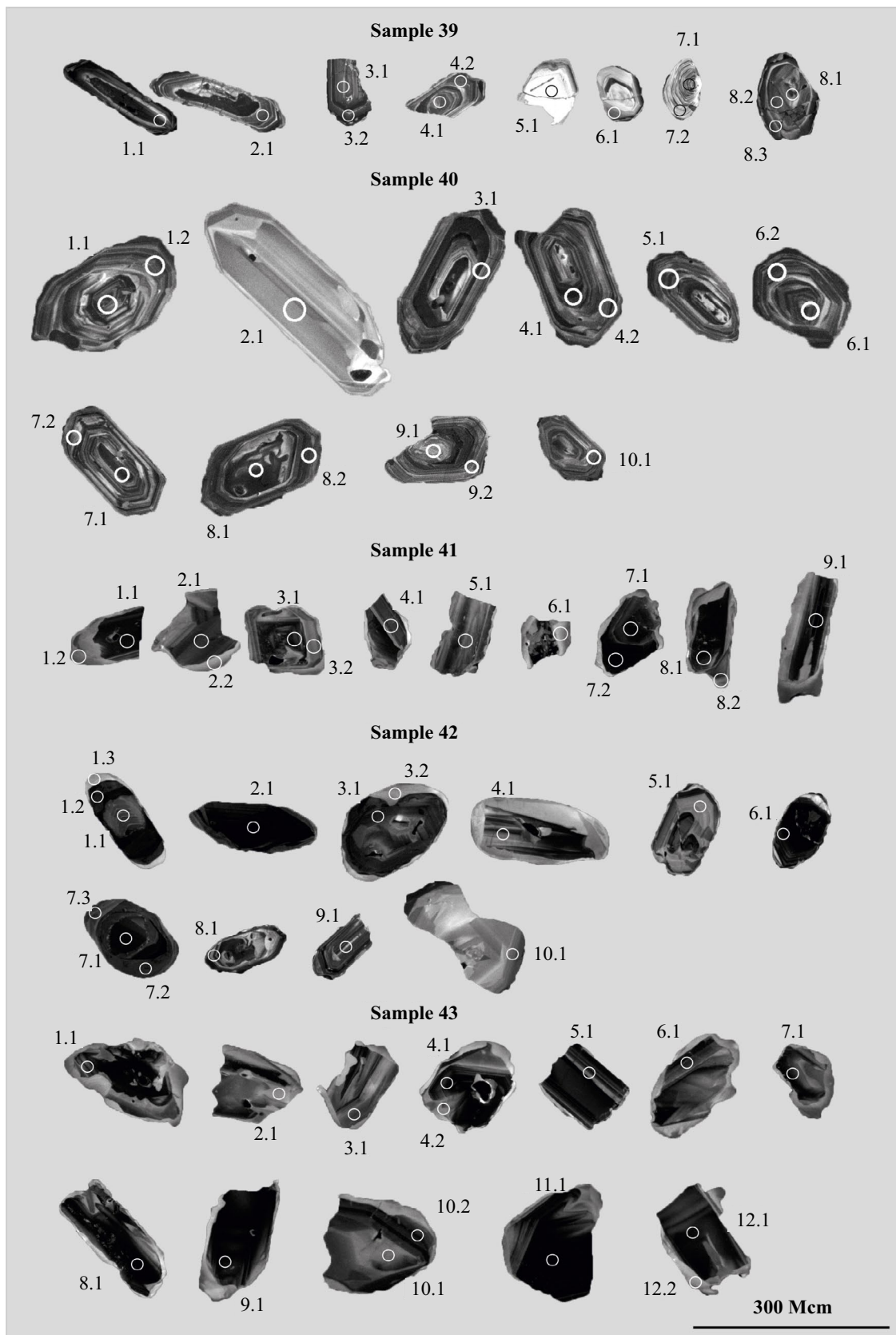


Fig. 3. Cathodoluminescence images of zircons from Eastern Mugodzhar eclogites, studied using SHRIMP II. (sample 42 – amphibolite). Circles show the location of measurement points, numbers correspond to analysis numbers in Table 1.

Table 1. U–Pb (SHRIMP II) isotopic data for zircons from Mugodzhari eclogites

Analysis No.	$^{206}\text{Pb}_c$, %	U, ppm	Th, ppm	$^{206}\text{Pb}^*$, ppm	$^{232}\text{Th}/^{238}\text{U}$	$^{207}\text{Pb}/^{235}\text{U}$, $\pm\%$	$^{206}\text{Pb}/^{238}\text{U}$, $\pm\%$	Rho	Age $^{206}\text{Pb}/^{238}\text{U}$, Ma
Sample 39									
1.1	0	262	215	17	0.85	0.618 ± 2.3	0.07549 ± 0.75	0.3	469.1 ± 3.4
2.1	0.15	456	221	29.9	0.5	0.621 ± 1.9	0.07622 ± 0.58	0.3	473.5 ± 2.6
3.1	0.19	324	122	21.4	0.39	0.585 ± 2.5	0.07658 ± 0.68	0.3	475.7 ± 3.1
3.2	0.49	973	372	63.4	0.39	0.591 ± 2	0.07544 ± 0.44	0.2	468.9 ± 2
4.1	0.74	422	229	27.5	0.56	0.584 ± 3.8	0.07526 ± 0.75	0.2	467.7 ± 3.4
4.2	0	487	220	31.8	0.47	0.613 ± 1.8	0.07596 ± 0.56	0.3	472 ± 2.6
5.1	0.28	70	31	4.98	0.45	0.674 ± 5.2	0.0826 ± 1.4	0.3	511.5 ± 6.7
6.1	0	223	82	16.1	0.38	0.684 ± 2.7	0.08405 ± 0.8	0.3	520.3 ± 4
7.1	0	314	181	22.4	0.6	0.659 ± 2.3	0.08318 ± 0.69	0.3	515.1 ± 3.4
7.2	0.2	105	54	7.51	0.53	0.671 ± 4.3	0.08333 ± 1.2	0.3	516 ± 5.8
8.1	4.52	271	151	21.6	0.58	0.705 ± 9.8	0.08815 ± 1	0.1	544.6 ± 5.3
8.2	0.15	353	222	23.3	0.65	0.584 ± 3	0.07678 ± 0.68	0.2	476.9 ± 3.1
8.3	0	453	61	24.8	0.14	0.528 ± 2.3	0.06372 ± 1.2	0.5	398.2 ± 4.7
Sample 40									
1.1	5.99	740	987	29.8	1.38	0.315 ± 9.1	0.04403 ± 1.7	0.2	277.7 ± 4.6
1.2	1.24	854	428	33.8	0.52	0.339 ± 3.7	0.04551 ± 1.1	0.3	286.9 ± 3.1
2.1	0	144	197	5.68	1.41	0.323 ± 4.1	0.04596 ± 1.5	0.4	289.6 ± 4.3
3.1	0.26	818	354	30.7	0.45	0.3142 ± 2.6	0.04356 ± 1.1	0.4	274.9 ± 3
4.1	0.1	1079	465	41.7	0.45	0.3175 ± 2.1	0.04497 ± 1.1	0.5	283.6 ± 3
4.2	0.06	1021	446	39.4	0.45	0.3251 ± 2	0.04488 ± 1.1	0.6	283 ± 3.1
5.1	0.14	797	607	30.2	0.79	0.3085 ± 2.4	0.04404 ± 1.1	0.5	277.8 ± 3
6.1	0	816	409	31.9	0.52	0.3265 ± 2	0.04554 ± 1.1	0.6	287.1 ± 3.2
6.2	0.42	1098	815	42.2	0.77	0.3226 ± 2.5	0.04452 ± 1.1	0.4	280.8 ± 2.9
7.1	3.39	1121	694	43.5	0.64	0.314 ± 9.9	0.0436 ± 1.2	0.1	275.1 ± 3.2
7.2	7.55	979	1133	34.7	1.2	0.252 ± 30	0.03817 ± 1.6	0.1	241.5 ± 3.8
8.1	0	2151	4080	83.8	1.96	0.3269 ± 1.4	0.04532 ± 1	0.7	285.7 ± 2.9
8.2	0.73	675	344	25.5	0.53	0.318 ± 3.8	0.04367 ± 1.1	0.3	275.5 ± 3.1
9.1	0.32	315	196	12.3	0.64	0.333 ± 4.1	0.0453 ± 1.3	0.3	285.6 ± 3.6
9.2	0.27	415	239	15.7	0.6	0.314 ± 3.4	0.04397 ± 1.2	0.4	277.4 ± 3.3
10.1	0	621	389	24.3	0.65	0.3219 ± 2.2	0.04545 ± 1.2	0.5	286.5 ± 3.3
Sample 41									
1.1	0	367	348	26.4	0.98	0.667 ± 2.3	0.08391 ± 0.72	0.3	519.4 ± 3.6
1.2	0.72	46	9	3.44	0.2	0.687 ± 9.2	0.0857 ± 1.9	0.2	530.1 ± 9.9
2.1	0.15	212	85	15.5	0.42	0.683 ± 3.2	0.08519 ± 0.91	0.3	527 ± 4.6
2.2	0	10	3	0.598	0.28	0.538 ± 15	0.0687 ± 4.9	0.3	429 ± 20
3.1	0	271	176	19.5	0.67	0.655 ± 2.8	0.08394 ± 0.96	0.3	519.6 ± 4.8
3.2	0	123	46	8.86	0.39	0.659 ± 4.2	0.0839 ± 1.2	0.3	519.6 ± 6.1
4.1	0	270	228	19.3	0.87	0.656 ± 2.8	0.08351 ± 0.95	0.3	517 ± 4.7

Ending

Analysis No.	$^{206}\text{Pb}_c$, %	U, ppm	Th, ppm	$^{206}\text{Pb}^*$, ppm	$^{232}\text{Th}/^{238}\text{U}$	$^{207}\text{Pb}/^{235}\text{U}$, $\pm\%$	$^{206}\text{Pb}/^{238}\text{U}$, $\pm\%$	Rho	Age $^{206}\text{Pb}/^{238}\text{U}$, Ma
5.1	0	99	46	7.16	0.48	0.674 ± 4.5	0.0842 ± 1.3	0.3	521.4 ± 6.7
6.1	0	2	1	0.0858	0.34	1.31 ± 27	0.0589 ± 12	0.5	369 ± 44
7.1	0.04	1183	521	87	0.46	0.6675 ± 1.4	0.08555 ± 0.52	0.4	529.2 ± 2.7
7.2	0	542	293	39	0.56	0.67 ± 1.9	0.08359 ± 0.61	0.3	517.5 ± 3
8.1	0.58	64	16	4.76	0.27	0.674 ± 7.6	0.0865 ± 1.7	0.2	535.1 ± 8.7
8.2	0.21	443	315	30.4	0.73	0.599 ± 3	0.07965 ± 0.7	0.2	494 ± 3.3
9.1	0	469	393	31.8	0.87	0.611 ± 2.2	0.07882 ± 0.77	0.3	489.1 ± 3.6

Sample 42

1.1	0.2	161	45	27.2	0.29	2.085 ± 2.5	0.1963 ± 0.91	0.4	1155.5 ± 9.6
1.2	5.06	11	0	0.594	0	0.34 ± 75	0.0619 ± 5.6	0.1	387 ± 21
1.3	0.34	395	3	20.7	0.01	0.478 ± 3.5	0.0609 ± 0.78	0.2	381.1 ± 2.9
2.1	0	701	350	51.5	0.52	0.675 ± 1.6	0.08553 ± 0.52	0.3	529 ± 2.7
3.1	0	180	55	12	0.32	0.604 ± 3.5	0.07783 ± 1.2	0.3	483.2 ± 5.5
3.2	0	11	0	0.587	0.02	0.538 ± 15	0.0625 ± 4.3	0.3	391 ± 16
4.1	0.11	219	243	16.5	1.14	0.688 ± 3.3	0.0875 ± 1.4	0.4	540.6 ± 7.2
5.1	0.39	84	51	7.65	0.63	0.887 ± 5.3	0.1062 ± 1.4	0.3	650.5 ± 8.5
6.1	0.83	594	301	25.4	0.52	0.37 ± 5.7	0.04937 ± 0.73	0.1	310.7 ± 2.2
7.1	0.08	494	633	48.8	1.33	0.99 ± 1.8	0.11504 ± 0.59	0.3	701.9 ± 3.9
7.2	0.13	288	4	14.8	0.01	0.474 ± 3.3	0.05981 ± 0.88	0.3	374.5 ± 3.2
7.3	0	206	2	10.9	0.01	0.483 ± 3.6	0.06169 ± 1	0.3	385.9 ± 3.8
8.1	0.15	346	135	22.6	0.4	0.6 ± 3.5	0.07617 ± 0.87	0.2	473.3 ± 4
9.1	0.19	214	130	14.1	0.63	0.595 ± 3.7	0.07688 ± 1.1	0.3	477.5 ± 5
10.1	0.18	207	87	10.6	0.44	0.433 ± 4.1	0.05939 ± 1	0.3	371.9 ± 3.7

Sample 43

1.1	0.13	176	64	13.1	0.37	0.664 ± 3.3	0.08644 ± 0.93	0.3	534.5 ± 4.7
2.1	0.72	32	7	2.3	0.24	0.637 ± 9.7	0.0836 ± 2.2	0.2	517 ± 11
3.1	0	91	28	6.47	0.31	0.68 ± 4.4	0.0826 ± 1.3	0.3	511.8 ± 6.4
4.1	0	1044	734	75	0.73	0.6643 ± 1.3	0.08361 ± 0.43	0.3	517.6 ± 2.2
4.2	0.47	47	13	3.41	0.28	0.65 ± 7.4	0.084 ± 1.8	0.2	520.2 ± 9
5.1	0.82	237	88	17.7	0.38	0.655 ± 4.9	0.08626 ± 0.84	0.2	533.4 ± 4.3
6.1	0.21	193	81	14.3	0.43	0.678 ± 3.5	0.08577 ± 1	0.3	530.5 ± 5.3
7.1	0	114	31	8.26	0.28	0.646 ± 4	0.08454 ± 1.2	0.3	523.2 ± 5.9
8.1	0.5	145	40	10.5	0.28	0.639 ± 5.7	0.08381 ± 1.1	0.2	518.8 ± 5.4
9.1	0.19	104	24	7.77	0.24	0.688 ± 5.1	0.0871 ± 1.4	0.3	538.5 ± 7.4
10.1	0.62	173	60	12.6	0.36	0.638 ± 5.7	0.08421 ± 1	0.2	521.2 ± 5
10.2	0	14	5	1	0.38	0.812 ± 9.8	0.0836 ± 3.5	0.4	517 ± 17
11.1	0.8	100	27	7.26	0.27	0.627 ± 7.6	0.0835 ± 1.3	0.2	516.7 ± 6.6
12.1	1.09	653	253	46.9	0.4	0.631 ± 3.3	0.08269 ± 0.56	0.2	512.1 ± 2.8
12.2	0	39	9	2.51	0.23	0.554 ± 7.7	0.0746 ± 2.1	0.3	463.8 ± 9.5

with epidote growing on their edges. Inclusions of allanite-(Ce) are found in glaucophane. *Titanite* in the rock occurs as inclusions together with rutile in almandine, omphacite, glaucophane, and in the aggregate of minerals of the epidote group. *Rutile* is found throughout the rocks both as separate grains of elongated or irregular shape and with titanite rims. Iron-enriched rutile (FeO up to 12.51 wt.%) occurs in the rocks. *Paragonite* forms small clusters of grains, partially replacing omphacite. In eclogites, cobalt-bearing *pyrite* (Co up to 2.46 wt.%) is noted as single grains in the almandine-amphibole aggregate. *Ilmenite* with high manganese content (MnO up to 4.71 wt.%) is found as an inclusion in almandine in eclogite together with rutile and titanite. *Albite* in rocks forms elongated grains in chamoisite-clinochlore aggregate together with phengite, muscovite, and calcite, as well as veinlets and accumulations with large glaucophane grains. *Quartz* in eclogites is present in small amounts as inclusions in garnet and calcite grains. *Fluorapatite* is noted as inclusions in almandine, omphacite, and calcite together with quartz. *Zircon* occurs as idiomorphic elongated grains up to 350 μm in size within rock-forming minerals.

U-PB SHRIMP DATING OF ECLOGITE ZIRCON

Sample 39 (Kitarsay complex). Eclogites (amphibolized, sometimes with plagioclase) in serpentinites. The thickness of eclogite bodies does not exceed 5 m. Their shape is elongated, boudin-like, up to 100 m in length. Zircons have a pink color, prismatic and elongated-prismatic habit (Fig. 3). The faces of crystals are shiny, the edges of some crystals are slightly rounded. The internal structure of the crystals is rhythmically zoned. In some crystals, an inner core is distinguished. Practically all obtained dates (Table 1) fall on the concordia (Fig. 4 A). Two clusters with concordant ages are distinguished on the concordia: 517 \pm 5 Ma (MSWD = 0.43), which corresponds to the Cambrian (Series 2, Stage 3, \approx 521–514 Ma, according to [17]) and 472 \pm 3 Ma (MSWD = 5.9) – corresponding to the Early Ordovician, Floian Stage. One analysis from the zircon core (Table 1, an. 8.1) showed an older date of 544.6 \pm 5.3 Ma.

Sample 40 (Kitarsay complex). Eclogite body among melanged serpentinites. The eclogites are amphibolized, especially at contacts with serpentinites. Serpentinites contain layers of intensely lightened (silicified) rocks, sometimes containing fuchsite. Among the eclogites, there are

granite veinlets, and banded albitized varieties of eclogites are also noted, in which leucocratic bands make up \approx 5%. Zircons in the rock form transparent pink prismatic and elongated-prismatic crystals with shiny faces (Fig. 3). The internal structure of the crystals is rhythmically zoned. In some crystals, a core part is observed. The obtained results gave a concordant age (Fig. 4 B, Table 1) of 282 \pm 2 Ma (MSWD = 0.2), which corresponds to the Early Permian time. One analysis of the edge part of the zircon showed a rejuvenated result of 241.5 \pm 3.8 million years (Table 1, sample 40, an. 7.2).

Sample 41 (Tulepsai complex) was collected from the right side of a small tributary of Tulepsai, in a drop-shaped eclogite boudin located among amphibolites with outcrop widths of more than 5 m. The eclogites are massive, medium-grained, and partially amphibolitized. The eclogites are conformably embedded in amphibolites. The amphibolites are platy, composed of muscovite-amphibole-garnet-feldspar; among accessory minerals, rutile strongly predominates, leucocratic interlayers constitute up to 35% of the rock volume. *Sample 42* was collected from the most massive and fresh amphibolites 3 m from the eclogite boudin. *Sample 43* from eclogites also located among amphibolites was taken 1.45 km southwest of sample 41.

Zircons from sample 41 eclogite are mainly represented by crystal fragments and short-prismatic crystals. The zircons are colorless and lightly pinkish with rounded edges and complex internal structure. Almost all zircons have a central core and zones with sectoriality and rhythmic zonation at the periphery (Fig. 3). Analyses were performed on the central and peripheral parts of the zircons (Table 1). Almost all the results obtained plot on the concordia (Fig. 4 B). The concordant age obtained for the zircons is 523 \pm 3 Ma (MSWD = 1.8), corresponds to the upper part of the Lower Cambrian (Stage 2). Analyses were made in the core, intermediate, and peripheral parts of the mineral grains. Four analyses gave younger ages: dates of 494, 489, and 429 Ma were obtained from the zone of later overgrowth of zircon crystals (Fig. 3, sample 41, an. 8.2, 9.1, 2.2). The point with analysis in the peripheral part of the zircon (Fig. 3, sample 41, an. 6.1) (\approx 369 Ma) deviated from the concordia.

Zircons from amphibolite sample 42. Different morphological types of zircon grains are observed in the sample. There are crystals of short-prismatic, elongated-prismatic dipyramidal habitus, and their fragments. Almost all grains have distinct shiny faces and are colorless. The sample also contains elongated grains with smoothed edges (Fig. 3).

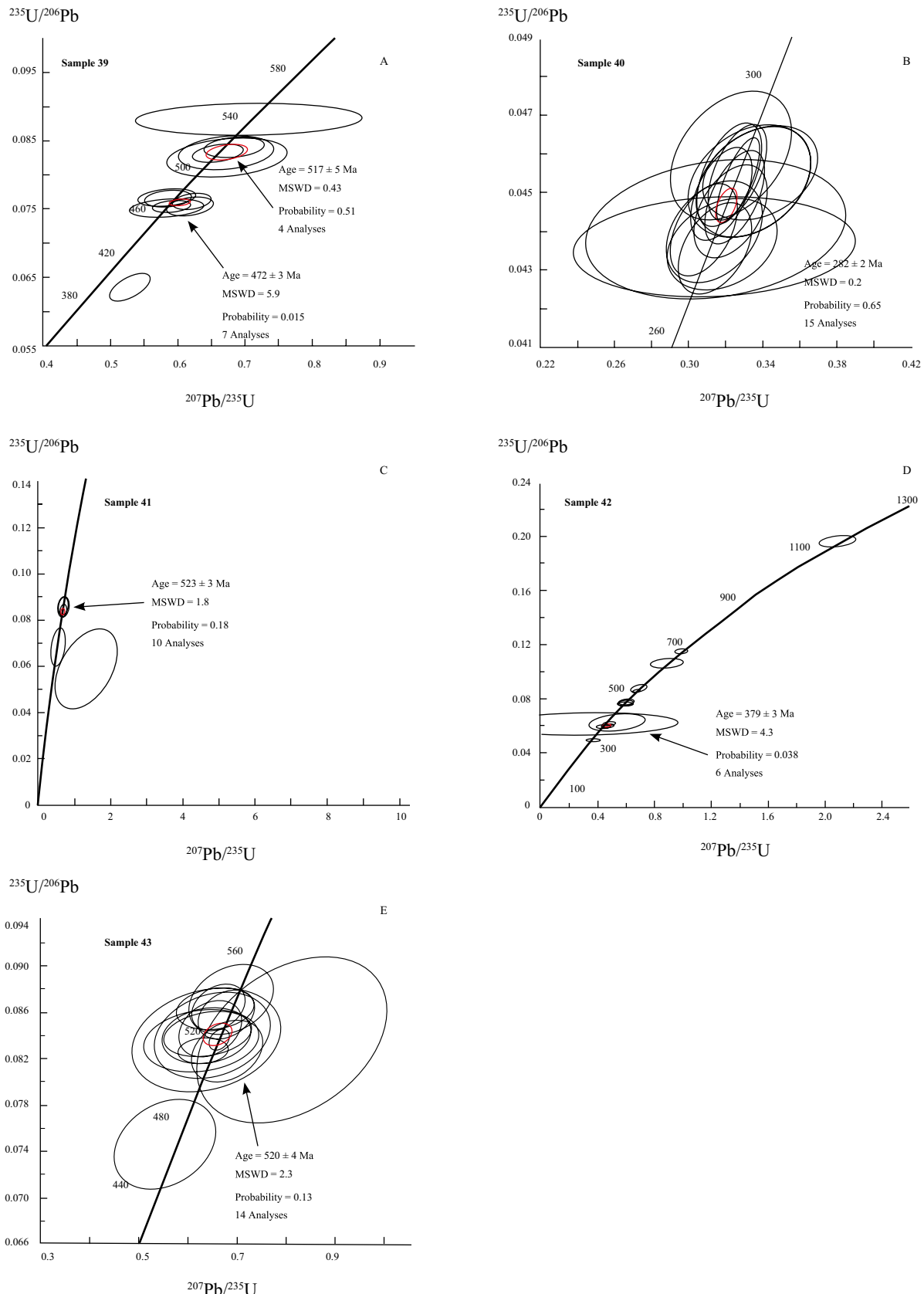


Fig. 4. Isotopic U-Pb concordia diagrams constructed from mass spectrometric study of zircon grains from Mugodzhari eclogites. A – sample 39; B – sample 40; C – sample 41; D – sample 42 (amphibolite); E – sample 43.

Crystals exhibit sectoriality and zonality. Zircons with a central, core part and subsequent overgrowth are observed. In the peripheral zones of four zircon grains, the concordant age (Fig. 4 G, Table 1) is 379 ± 3 Ma (MSWD = 4.3), corresponding to the Frasnian stage.

Zircons from eclogite sample 43 are represented by elongated crystals and their fragments (Fig. 3). The crystals have rounded edges, dissolution traces, and are colorless. Within the crystals, a core part and a peripheral part are noted. Rhythmic zonality is observed in the peripheral zone of the grains. The obtained results (Table 1, Fig. 4 D) gave a concordant age of 520 ± 4 Ma (MSWD = 2.3). A younger age of 464 Ma was obtained from the edge of one zircon fragment.

DISCUSSION OF RESULTS AND CONCLUSIONS

The metamorphic rocks we studied, represented predominantly by omphacite with up to 47% of jadeite mineral, glaucophane and almandine containing up to 18% of pyrope mineral, as well as paragonite, clinozoisite, a large amount of accessory rutile, judging by the association, are fairly typical eclogites that underwent retrograde metamorphism with the formation of a large amount of Na-amphibole and albite-actinolite symplectites.

The results of isotopic U-Pb dating of zircons from the eclogites of the Eastern Mugodzhari showed a very complex history of their formation and transformation, the detailed decoding of which will apparently be possible only in the future, with the use of other isotope-geochronometric systems (Rb-Sr, Sm-Nd, etc.). However, the data presented in the article already prove the main point that the metamorphic complexes of the Mugodzhars are not Early Proterozoic or Riphean formations (as previously thought), but represent Lower-Middle Paleozoic complexes of the middle part of the Earth's crust. That is, these metamorphites are not the once-assumed Madagascar-type microcontinent [7], nor part of the foundation of the Russian platform [14], but are fragments of the deep part of the island arc system of the eastern sector of the Urals, which later (in the Middle-Late Triassic) were brought to a near-surface level during the uplift and erosion of certain areas of the Urals (for more details, see [6]). It should be noted that in the rocks of the eastern (paleo-island arc) sector of the Urals (i.e., east of the Main Uralian Fault), not a single reliable pre-Paleozoic dating is known today [5].

Of the 4 eclogite samples, samples 39, 41, and 43 have similar (and the “oldest”) concordant age values with dates of 517 ± 5 Ma, 523 ± 3 Ma, and 520 ± 4 Ma, respectively. The obtained age (average 520 ± 4 Ma) approximately corresponds to the upper boundary of the Early Cambrian (Terreneuvian Series) [17] and probably *corresponds to the age of the protolith*. And although Cambrian formations in the Urals are poorly preserved, Cambrian basalts are known, for example, in the Sakmara zone of the Southern Urals, near the city of Mednogorsk [12].

The youngest zircons from the eclogites of Mugodzhari have a clearly manifested age of 282 ± 2 Ma (Early Permian, sample 40), apparently corresponding to the stage of collision and associated granite massifs [2, 3]. In this case, this is also the age of formation of the Bugetsai fault.

The other two concordant dates: 472 ± 3 Ma (Lower-Middle Ordovician, sample 39) and 379 ± 3 Ma (Frasnian age, sample 42), obviously reflect the time of the main stages of metamorphism. As noted in [15], the “Frasnian” age of the Mugodzhari metamorphites coincided with the age of the main phase of high-pressure metamorphism in the zone of the Main Ural deep fault in the Southern Urals (Maksyutov complex, see [18]), as well as with the age of high-grade metamorphites in the northeast of the Middle Urals (Salda complex, see [11]). The Salda complex, although located 1100 km to the north, is in the same zone as the considered metamorphites of the Eastern Mugodzhari. The data presented above force us to consider the Frasnian age of the amphibolite facies metamorphism of the Eastern Mugodzhari. This also corresponds to the information [8] that the age of newly formed (i.e., not clastic) zircons in biotite-bearing quartz-feldspar gneisses of the South Mugodzhari series was also 373 ± 4 Ma. The concordant dating of 472 ± 3 Ma (sample 39), according to our data, corresponds to the age of high-pressure metamorphism of Mugodzhari.

We note that in sample 42 (amphibolites), the core parts of 4 crystals gave ancient dates of 1155, 702, and 483 Ma. The central zones of zircons with smoothed edges have ages of 650, 541, and 529 Ma. Two zircons of prismatic habit showed similar ages of 471 and 478 Ma. The presence of ancient and diverse-aged zircons, apparently with traces of rounding, indicates the primary sedimentary nature of the amphibolite in this sample.

ACKNOWLEDGEMENTS

For their help and support, the authors express their sincere gratitude to colleagues Yu.V. Erokhin, L.A. Karsten, and I.A. Pelevin (IGG RAS), as well as to A.N. Larionov from the VSEGEI IRC (St. Petersburg) for conducting zircon analyses, and to the anonymous reviewer for comments that helped improve the article.

FUNDING

The work was carried out within the framework of the topic No. 123011800014-3 of the state assignment of the IGG UB RAS.

REFERENCES

1. *Biryukov V.M.* High-pressure complexes of mobile belts. Moscow: Nauka, 1988. 208 p.
2. Geological map of the Kazakh SSR. Scale 1:500,000. Turgai-Mugodzhari Series. Alma-Ata. 1981. 228 p.
3. *Golionko B.G., Ryazantsev A.V.* Deformations and structural evolution of metamorphic complexes of the Taldyk antiform of the East Mugodzhari zone of the Urals (Western Kazakhstan) // Geodynamics and Tectonophysics. 2021. Vol. 12. No. 1. P. 48–59.
4. *Efimov I.A., Burd G.I.* Regional metamorphism, age and formation conditions of some deep Precambrian rocks of Mugodzhari // Soviet Geology. 1970. No. 11. P. 36–56.
5. *Ivanov K.S., Panov V.F., Likhanov I.I., Kozlov P.S., Ponomarev V.S., Hiller V.V.* Precambrian of the Urals // Mining Bulletin. 2016. Vol. 148. No. 9. P. 4–21.
6. *Ivanov K.S., Puchkov V.N.* Structural-formational zones of the Ural folded belt: review of data and development of new ideas // Geotectonics. 2022. No. 6. P. 78–113.
7. *Ivanov S.N., Puchkov V.N., Ivanov K.S., Samarkin G.I., Semenov I.V., Pumpyansky A.I., Dymkin A.M., Poltavets Yu.A., Rusin A.I., Krasnobaev A.A.* Formation of the Earth's crust in the Urals. Moscow: Nauka. 1986. 246 p.
8. *Krasnobaev A.A., Bayanova T.B.* New data on zircon geochronology of the Taldyk block of Mugodzhary // Yearbook-2005. Yekaterinburg: IGG UB RAS. 2006. P. 297–300.
9. *Krasnobaev A.A., Davydov V.A.* Zircon geochronology of the Taldyk block of Mugodzhary // Reports of the Academy of Sciences. 1999. Vol. 366. No. 1. P. 95–99.
10. *Milovsky A.V., Getling R.V., Zverev A.T., Roshkovan G.R., Svalnova V.I.* Precambrian and Lower Paleozoic of Western Kazakhstan. Moscow: MSU. 1977. 268 p.
11. *Petrov G. A., Ronkin Yu.L., Maslov A.V., Svyazhina I.A., Rybalka A.V., Lepikhina O.P.* The timing of the beginning of collision in the Middle and Northern Urals. // DAN. 2008. Vol. 422. No. 3. P. 365–370.
12. *Puchkov V.N.* Paleogeodynamics of the Southern and Middle Urals. Ufa: Gilem, 2000. 146 p.
13. *Rusin A.M.* Kitarsai Eclogite-Peridotite Association of Mugodzhari // Yearbook-1995. Yekaterinburg: IGG UB RAS. 1996. P. 99–103.
14. *Rusin A.I.* Metamorphic Complexes of the Urals and the Problem of Metamorphism Evolution in the Complete Cycle of Lithosphere Development in Mobile Belts. Abstract of dissertation for the degree of Doctor of Geological and Mineralogical Sciences. Yekaterinburg: IGG UB RAS. 2004. 46 p.
15. *Ryazantsev A.V., Golionko B.G., Kotov A.B., Skoblenko A.V., Stifeeva M.V., Plotkina Yu.V., Salnikova E.B., Koreshkova M.Yu., Machev F.* Age and Thermal History of Eclogites from the Tulepsai Complex of the Eastern Mugodzhari (Western Kazakhstan) // Doklady RAS. Earth Sciences. 2022. Vol. 506. No. 1. P. 5–13.
16. *Yurish V.V., Ulukpanov K.T.* Geodynamics of the Paleozoic of the Kazakh Urals. Aktobe: AKTYUBNIGRI LLP. 2020. 365 p.
17. *Cohen K.M., Harper D.A.T., Gibbard P.L., Carr N.* The ICS International Chronostratigraphic Chart, February 2022. Available from: <http://www.stratigraphy.org/ ICSchart/ChronostratChart2022-02.pdf>.
18. *Glodny J., Bingen B., Austrheim H., Molina J.F., Rusin A.* Precise Eclogitization Ages Deduced from Rb/Sr Mineral Systematics: The Maksyutov Complex, Southern Urals, Russia // Geoch. Acta. 2002. V. 66 (7). P. 1221–1235.
19. *Ludwig K.R.* ISOPLOT 3.00. A User's Manual // Berkeley Geochronology Center Special Publication. 2003. № 4. 2455 RidgeRoad, Berkeley. CA 94709. USA. 70 p.
20. *Williams I.S.* U–Th–Pb geochronology by ion microprobe. Applications of microanalytical techniques to understanding mineralizing processes // Rev. Econ. Geol. 1998. V. 7. P. 1–35.

**APPENDIX 1. CHEMICAL COMPOSITION OF MINERALS
FROM MUGODZHAR ECLOGITES (KAZAKHSTAN)**

The chemical composition of minerals was determined using a Camebax SX50 X-ray microanalyzer (Department of Mineralogy, Faculty of Geology, Moscow State University, analyst D. A. Khanin) at an accelerating voltage of 15 kV and a probe current of 30 nA. The corresponding phosphates were used as standards for REE, for Na, Si – chkalovite, Mg, Ca, Fe – hornblende, Al – albite, K – orthoclase, Ti – KTiPO_5 synth., Cr – magnesiochromite, V – vanadium, MnTiO_5 , Co – cobaltin, Ni – NiO , Sr – celestine, Ba – barite. Water content was not carried out by direct method.

Table 1. Chemical composition (in wt.%) of minerals from eclogites

No.	SiO_2	TiO_2	Al_2O_3	V_2O_5	MgO	FeO	MnO	SrO	CaO	Na_2O	K_2O	Amount
Almandine												
1	37.86	—	21.83	—	4.50	31.15	0.34	—	4.33	—	—	100.01
2	37.69	—	21.60	—	3.04	32.38	0.56	—	4.73	—	—	100.00
3	37.81	—	21.56	—	3.51	29.00	0.19	—	7.56	—	—	99.63
4	38.07	0.15	21.66	—	2.32	28.22	0.28	—	9.30	—	—	100.00
5	38.04	0.23	21.87	—	3.16	27.30	0.24	—	9.16	—	—	100.00
6	38.16	—	21.88	—	4.43	28.86	0.20	—	6.47	—	—	100.00
7	37.75	—	21.72	—	4.32	31.06	0.45	—	4.71	—	—	100.01
8	38.03	0.16	21.65	—	3.24	27.65	0.20	—	9.06	—	—	99.99
9	37.98	—	21.75	—	3.59	28.74	0.22	—	7.72	—	—	100.00
10	37.54	0.39	21.03	—	3.13	27.78	0.84	—	9.18	—	—	99.89
11	37.14	0.20	20.96	—	2.91	28.62	0.87	—	9.08	—	—	99.78
12	38.12	0.39	21.23	—	3.84	28.30	0.62	—	8.87	—	—	101.37
13	37.57	—	21.06	—	3.12	29.63	1.11	—	7.84	—	—	100.33
14	37.90	—	21.17	—	4.35	31.08	0.67	—	5.12	—	—	100.29
Glaucophane												
15	58.16	—	11.71	—	10.69	8.92	0.05	—	0.32	7.77	—	97.62
16	57.92	—	11.36	—	10.62	9.44	—	—	0.74	7.72	—	97.80
17	57.85	—	11.50	—	9.58	10.72	—	—	0.19	7.88	—	97.72
18	56.59	—	10.89	—	11.17	9.59	—	—	1.58	7.31	—	97.13
19	56.10	0.11	11.37	—	10.14	10.63	—	—	1.56	7.25	—	97.16
Omphacite												
20	56.88	—	10.04	0.10	8.37	5.05	—	—	13.22	6.64	—	100.30
21	56.83	—	10.52	—	8.86	4.44	—	—	13.62	7.21	—	101.48
22	57.00	0.11	10.05	—	7.91	5.40	—	—	12.57	6.63	—	99.67
23	56.19	0.07	11.02	0.10	8.32	5.53	0.06	—	12.76	7.16	—	101.21
24	55.85	—	10.11	0.10	8.54	4.99	—	—	13.22	7.25	—	100.06
25	55.58	0.10	10.98	0.09	7.20	5.63	0.07	—	12.09	7.96	—	99.70
26	54.96	0.23	11.95	0.15	6.44	6.41	0.05	—	10.24	8.58	—	99.01
27	55.99	0.16	11.49	—	7.40	6.08	—	—	10.48	8.33	—	99.93
28	56.48	0.18	11.23	0.11	7.04	6.03	0.09	—	11.31	8.42	—	100.89
29	56.72	0.25	11.94	0.08	7.00	5.48	—	—	10.93	8.63	—	101.03

Ending

No.	SiO ₂	TiO ₂	Al ₂ O ₃	V ₂ O ₅	MgO	FeO	MnO	SrO	CaO	Na ₂ O	K ₂ O	Amount
Actinolite												
30	51.81	0.09	4.39	0.11	11.46	18.13	0.28	—	10.71	1.63	0.14	98.75
31	50.73	0.07	4.24	0.24	12.10	17.86	0.29	0.09	11.58	1.21	0.11	98.28
Amphiboles of a number of ferropargasite–ferroedenite												
32	41.45	0.25	12.29	0.19	4.64	26.09	0.25	—	10.56	2.94	0.35	99.01
33	41.03	0.14	11.7	0.09	4.54	25.97	0.21	—	10.29	2.87	0.35	97.19
34	42.69	0.05	9.96	0.00	5.56	25.82	0.26	—	10.83	2.52	0.36	98.05
Chlorite												
35	24.66	0.79	19.25	—	10.80	29.72	0.23	—	0.81	0.18	—	86.44
36	26.06	0.26	16.16	—	11.12	31.27	0.38	0.29	0.54	0.22	—	86.30
37	28.27	—	19.25	0.12	23.95	13.79	0.09	—	0.10	0.08	—	85.65
38	28.99	—	19.49	—	23.58	14.50	—	—	0.24	0.14	—	86.94
Muscovite												
39	50.50	0.30	27.00	0.16	3.32	2.57	—	—	0.11	0.71	11.05	95.72
40	50.62	0.25	27.10	0.12	3.31	2.63	—	—	—	0.68	10.89	95.60
Zoisite												
41	39.56	—	32.40	0.10	0.06	1.08*	—	0.16	24.58	—	—	97.94
42	39.22	0.05	31.69	0.22	—	2.81*	—	0.42	24.04	0.07	—	98.52
Clinozoisite–epidote												
43	37.73	0.11	26.63	0.12	—	7.90*	0.11	0.00	23.21	0.06	—	95.87
44	38.20	0.00	25.93	0.41	—	9.49*	0.10	0.16	23.56	0.00	—	97.85
Paragonite												
45	47.46	0.00	37.00	0.11	0.89	0.56	—	—	0.16	7.66	0.94	94.78
46	46.68	0.11	37.48	0.33	0.50	0.64	—	—	0.10	7.25	1.22	94.31
Titanite												
47	30.44	37.48	1.48	0.77	—	0.27	—	0.06	28.59	0.08	—	99.17
48	30.59	38.13	1.61	0.50	—	0.24	0.08	0.14	28.67	0.05	—	100.01
Rutile												
49	0.16	97.63	0.07	0.97	—	1.03	—	—	—	—	—	99.86
50		98.11	0.07	2.07	—	0.25	—	—	—	—	—	100.50
51	—	86.42	—	0.81	—	12.51	1.27	—	—	—	—	101.01
Ilmenite												
52	0.26	53.89	0.12	0.34	—	39.80	4.71	—	0.25	—	—	99.37
Albite												
53	67.32	—	19.10	—	—	0.68	—	—	0.15	12.21.21	—	99.46.46
54	69.13.13	—	19.12.12	—	—	0.54.54	—	—	0.27.27	11.67.67	—	100.73.73
Calcite												
55	0.34.34	—	—	—	—	1.55.55	0.46.46	0.14.14	50.50.50	—	—	52.99.99
56	—	—	—	—	—	0.74.74	0.41.41	0.08.08	51.48.48	—	—	52.71.71

Note: here and in Table 2 – analyses: 32, 33 – ferropargasite; 34 – ferroedenite; 35, 36 – chamosite; analyses 37, 38 – clinochlore. BAn. 3 – additionally determined Cr₂O₃ 0.37.37 wt.% (0.02 f.u.).

* – the content of Fe₂O₃ in the mineral

Table 2. Crystal chemical recalculations (in f.u.) of minerals from eclogites

No	Si	Ti	Al	V	Mg	Fe ²⁺	Fe ³⁺	Mn	Sr	Ca	Na	K
Almandine												
1	2.99	—	2.03	—	0.53	2.06	—	0.02	—	0.37	—	—
2	3.01	—	2.03	—	0.36	2.16	—	0.04	—	0.40	—	—
3	2.99	—	2.01	—	0.41	1.92	—	0.01	—	0.64	—	—
4	3.02	0.01	2.02	—	0.27	1.87	—	0.02	—	0.79	—	—
5	3.00	0.01	2.03	—	0.37	1.80	—	0.02	—	0.77	—	—
6	3.00	—	2.03	—	0.52	1.90	—	0.01	—	0.55	—	—
7	2.98	—	2.02	—	0.51	2.05	0.01	0.03	—	0.40	—	—
8	3.00	0.01	2.01	—	0.38	1.82	—	0.01	—	0.77	—	—
9	3.00	—	2.02	—	0.42	1.90	—	0.02	—	0.65	—	—
10	2.97	0.02	1.96	—	0.37	1.79	0.05	0.06	—	0.78	—	—
11	2.95	0.01	1.96	—	0.35	1.79	0.12	0.06	—	0.77	—	—
12	2.97	0.02	1.95	—	0.45	1.76	0.08	0.04	—	0.74	—	—
13	2.97	—	1.96	—	0.37	1.87	0.10	0.07	—	0.66	—	—
14	2.99	—	1.97	—	0.51	2.00	0.05	0.05	—	0.43	—	—
Glaucophane												
15	7.93	—	1.88	—	2.17	0.91	0.11	0.01	—	0.05	2.05	—
16	7.91	—	1.83	—	2.16	0.93	0.15	—	—	0.11	2.04	—
17	7.94	—	1.86	—	1.96	1.12	0.11	—	—	0.03	2.10	—
18	7.81	—	1.77	—	2.30	0.87	0.24	—	—	0.23	1.96	—
19	7.78	0.01	1.86	—	2.10	1.03	0.20	—	—	0.23	1.95	—
Omphacite												
20	2.02	—	0.42	—	0.44	0.15	—	—	—	0.50	0.46	—
21	1.98	—	0.43	—	0.46	0.04	0.09	—	—	0.51	0.49	—
22	2.04	—	0.43	—	0.42	0.16	—	—	—	0.48	0.46	—
23	1.97	—	0.46	—	0.44	0.08	0.08	—	—	0.48	0.49	—
24	1.98	—	0.42	—	0.45	0.03	0.12	—	—	0.50	0.50	—
25	1.98	—	0.46	—	0.38	0.04	0.13	—	—	0.46	0.55	—
26	1.97	0.01	0.50	—	0.34	0.05	0.15	—	—	0.39	0.60	—
27	1.98	—	0.48	—	0.39	0.00	0.13	0.18	—	0.40	0.57	—
28	1.98	0.01	0.47	—	0.37	0.05	0.13	—	—	0.43	0.57	—
29	1.98	0.01	0.49	—	0.37	0.05	0.12	—	—	0.41	0.59	—
Actinolite												
30	7.51	0.01	0.75	0.01	2.48	1.80	0.40	0.03	—	1.66	0.46	0.03
31	7.43	0.01	0.73	—	2.64	1.89	0.30	0.04	0.01	1.82	0.34	0.02

Ending

No	Si	Ti	Al	V	Mg	Fe ²⁺	Fe ³⁺	Mn	Sr	Ca	Na	K
Amphiboles of a number of ferropargasite–ferroedenite												
32	6.36	0.03	2.22	0.02	1.06	2.92	0.43	0.03	—	1.74	0.87	0.07
33	6.41	0.02	2.16	0.01	1.06	2.94	0.45	0.03	—	1.72	0.87	0.07
34	6.61	0.01	1.82	—	1.28	3.01	0.34	0.03	—	1.80	0.76	0.07
Chlorite												
35	2.73	0.07	2.51	—	1.78	2.75	—	0.02	—	0.10	0.04	—
36	3.00	0.02	2.19	—	1.91	2.71	—	0.04	—	0.07	0.05	—
37	2.87	—	2.30	0.01	3.62	1.17	—	0.01	—	0.01	0.02	—
38	2.94	—	2.33	—	3.57	1.11	—	—	—	0.03	0.03	—
Muscovite												
39	3.38	0.02	2.13	0.01	0.33	0.14	—	—	—	0.01	0.09	0.94
40	3.39	0.01	2.14	0.01	0.33	0.15	—	—	—	—	0.09	0.93
Zoisite												
41	3.01	—	2.91	0.01	0.01	—	0.06	—	0.01	2.00	—	—
42	2.99	—	2.85	0.01	—	—	0.16	—	0.02	1.96	—	—
Clinozoisite–epidote												
43	3.01	0.01	2.50	0.01	—	—	0.47	0.01	—	1.98	0.01	—
44	3.01	—	2.41	0.02	—	—	0.56	0.01	0.01	1.99	—	—
Paragonite												
45	3.04	—	2.80	0.01	0.09	0.03	—	—	—	0.01	0.95	0.08
46	3.02	0.01	2.86	0.01	0.05	0.04	—	—	—	0.01	0.91	0.10
Titanite												
47	0.99	0.92	0.06	0.02	—	—	—	—	—	1.00	0.01	—
48	0.99	0.93	0.06	0.01	—	—	—	—	—	1.00	—	—
Rutile												
49	—	0.98	—	0.01	—	0.01	—	—	—	—	—	—
50	—	0.97	—	0.02	—	—	—	—	—	—	—	—
51	—	0.84	—	0.01	—	0.14	0.01	—	—	—	—	—
Ilmenite												
52	0.01	1.03	—	0.01	—	0.85	0.10	—	—	0.01	—	—
Albite												
53	2.95	—	0.99	—	—	0.03	—	—	—	0.01	1.04	—
54	3.01	—	0.98	—	—	0.02	—	—	—	0.01	0.98	—
Calcite												
55	0.01	—	—	—	—	0.02	0.01	—	—	0.96	—	—
56	—	—	—	—	—	0.01	0.01	—	—	0.98	—	—

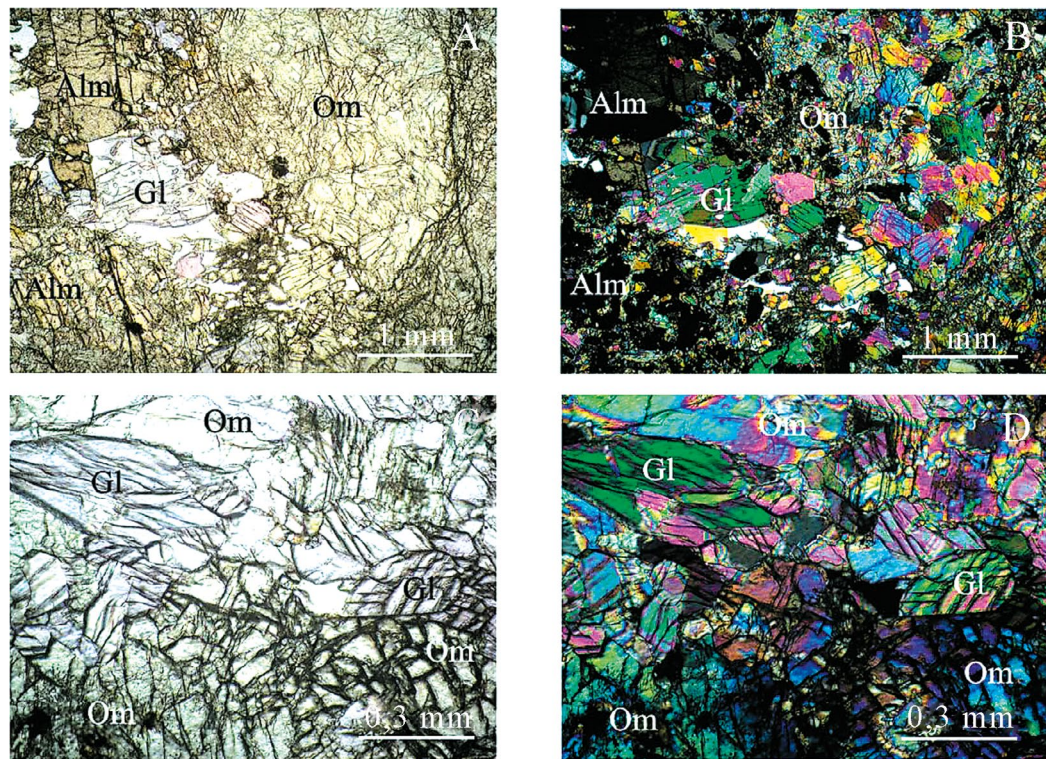


Fig. Eclogite of the Tulepsay complex of Eastern Mugodzhary (sample 43). In transmitted light (A), in polarized light (B). Omphacite and glaucophane from eclogite (sample 43); in transmitted light (C), in polarized light (D). Alm – almandine, Om – omphacite, Gl – glaucophane.